J|A|C|S
ARTICLES
Published on Web 02/10/2006

Using a Kinase/Phosphatase Switch to Regulate a Supramolecular Hydrogel and Forming the Supramolecular Hydrogel in Vivo

Zhimou Yang, Gaolin Liang, Ling Wang, and Bing Xu*,†

Contribution from the Department of Chemistry and Bioengineering Program, The Hong Kong University of Science and Technology, Clear Water Bay, Hong Kong, China

Received October 31, 2005; Revised Manuscript Received January 15, 2006; E-mail: chbingxu@ust.hk

Abstract: We have designed and synthesized a new hydrogelator Nap−FFGEY (**1**), which forms a supramolecular hydrogel. A kinase/phosphatase switch is used to control the phosphorylation and dephosphorylation of the hydrogelator and to regulate the formation of supramolecular hydrogels. Adding a kinase to the hydrogel induces a gel−sol phase transition in the presence of adenosine triphosphates (ATP) because the tyrosine residue is converted into tyrosine phosphate by the kinase to give a more hydrophilic molecule of Nap−FFGEY−P(O)$(OH)_2$ (**2**); treating the resulting solution with a phosphatase transforms **2** back to **1** and restores the hydrogel. Electron micrographs of the hydrogels indicate that **1** self-assembles into nanofibers. Subcutaneous injection of **2** in mice shows that 80.5 ± 1.2% of **2** turns into **1** and results in the formation of the supramolecular hydrogel of **1** in vivo. This simple biomimetic approach for regulating the states of supramolecular hydrogels promises a new way to design and construct biomaterials.

Introduction

This article reports a general strategy to control the states of a supramolecular hydrogel via an enzymatic switch[1] and in vivo formation of the supramolecular hydrogel. As one of the most utilized biomaterials in drug delivery, wound healing, and tissue engineering, hydrogels usually use natural or synthetic polymers as the gelators.[2] Largely because of the study of low molecular weight organogelators[3] and the demonstration of hydrogels made of self-assembled oligopeptides as scaffolds for tissue engineering,[4−6] the range of hydrogelators has expanded rapidly to include small molecules (which make possible supramolecular hydrogels) in the past decade.[7−9] The self-assembly of the hydrogelators plays a key role during the process of gelation in a supramolecular hydrogel.[7] Therefore, triggering or regulating the self-assembly of hydrogelators becomes an essential step in controlling the states and properties of supramolecular hydrogels, which is normally achieved by chemical or physical perturbations (e.g., pH, temperature, ionic strength, and ultrasonic agitation). In biomedical applications, enzyme-catalyzed, in situ reversible self-assembly and gelation of the hydrogelators is advantageous[10] because it allows the hydrogels to respond to the expressions of specific enzymes for certain tissues, organs, or diseases. Despite the use of an enzyme to cross-link polymers to induce hydrogelation[11] and reports on an enzyme-triggered formation of supramolecular hydrogels,[9] the use of enzymes to

* To whom correspondence should be addressed. Phone: 0852-2358-7351. Fax: 852-2358-1594.
† Bioengineering Program.

(1) Lodish, H. *Molecular Cell Biology*, 5th ed.; W. H. Freeman Co.: New York, 2003.
(2) Lee, K. Y.; Mooney, D. J. *Chem. Rev.* **2001**, *101*, 1869−79. Langer, R. *Nature* **1998**, *392*, 5−10. Tang, M. D.; Golden, A. P.; Tien, J. *J. Am. Chem. Soc.* **2003**, *125*, 12988−89.
(3) Terech, P.; Weiss, R. G. *Chem. Rev.* **1997**, *97*, 3133−59. de Loos, M.; van Esch, J.; Stokroos, I.; Kellogg, R. M.; Feringa, B. L. *J. Am. Chem. Soc.* **1997**, *119*, 12675−76. Ostuni, E.; Kamaras, P.; Weiss, R. G. *Angew. Chem., Int. Ed.* **1996**, *35*, 1324−26. Jung, J. H.; Ono, Y.; Hanabusa, K.; Shinkai, S. *J. Am. Chem. Soc*. **2000**, *122*, 5008−09. Shirakawa, M.; Fujita, N.; Shinkai, S. *J. Am. Chem. Soc.* **2003**, *125*, 9902−03. Xing, B. G.; Choi, M. F.; Xu, B. *Chem Commun.* **2002**, 362−63. Xing, B. G.; Choi, M. F.; Xu, B. *Chem.−Eur. J.* **2002**, *8*, 5028−32.
(4) Silva, G. A.; Czeisler, C.; Niece, K. L.; Beniash, E.; Harrington, D.; Kessler, J. A.; Stupp, S. I. *Science* **2004**, *303*, 1352−55.
(5) Holmes, T. C.; de Lacalle, S.; Su, X.; Liu, G. S.; Rich, A.; Zhang, S. G. *Proc. Natl. Acad. Sci. U.S.A.* **2000**, *97*, 6728−33. Zhang, S. G. *Nat. Biotechnol.* **2003**, *21*, 1171−78. Niece, K. L.; Hartgerink, J. D.; Donners, J.; Stupp, S. I. *J. Am. Chem. Soc.* **2003**, *125*, 7146−47.
(6) Behanna, H. A.; Donners, J. J. J. M.; Gordon, A. C.; Stupp, S. I. *J. Am. Chem. Soc.* **2005**, *127*, 1193−200.
(7) Estroff, L. A.; Hamilton, A. D. *Chem. Rev.* **2004**, *104*, 1201−17. de Loos, M.; Feringa, B. L.; van Esch, J. H. *Eur. J. Org. Chem.* **2005**, 3615−31.
(8) Sreenivasachary, N.; Lehn, J. M. *Proc. Natl. Acad. Sci. U.S.A.* **2005**, *102*, 5938−43. Yoshimura, I.; Miyahara, Y.; Kasagi, N.; Yamane, H.; Ojida, A.; Hamachi, I. *J. Am. Chem. Soc.* **2004**, *126*, 12204−05. Hirst, A. R.; Smith, D. K. *Chem.−Eur. J.* **2005**, *11*, 5496−508. Estroff, L. A.; Hamilton, A. D. *Angew. Chem., Int. Ed.* **2000**, *39*, 3447−50. Menger, F. M.; Caran, K. L. *J. Am. Chem. Soc.* **2000**, *122*, 11679−91. Kiyonaka, S.; Sugiyasu, K.; Shinkai, S.; Hamachi, I. *J. Am. Chem. Soc.* **2002**, *124*, 10954−55. Bommel, V.; C., K. J.; Stuart, M. C. A.; Feringa, B. L.; Van Esch, J. *Org. Biomol. Chem.* **2005**, *3*, 2917−20. Kiyonaka, S.; Sada, K.; Yoshimura, I.; Shinkai, S.; Kato, N.; Hamachi, I. *Nat. Mater.* **2004**, *3*, 58−64. Bhuniya, S.; Park, S. M.; Kim, B. H. *Org. Lett.* **2005**, *7*, 1741−44. Xing, B. G.; Yu, C. W.; Chow, K. H.; Ho, P. L.; Fu, D. G.; Xu, B. *J. Am. Chem. Soc.* **2002**, *124*, 14846−47. Zhang, Y.; Gu, H.; Yang, Z.; Xu, B. *J. Am. Chem. Soc.* **2003**, *125*, 13680−81. Zhang, Y.; Yang, Z. M.; Yuan, F.; Gu, H. W.; Gao, P.; Xu, B. *J. Am. Chem. Soc.* **2004**, *126*, 15028−29. Yang, Z. M.; Gu, H. W.; Zhang, Y.; Wang, L.; Xu, B. *Chem. Commun.* **2004**, 208−09. Yang, Z. M.; Xu, K. M.; Wang, L.; Gu, H. W.; Wei, H.; Zhang, M. J.; Xu, B. *Chem. Commun.* **2005**, 4414−16.
(9) Yang, Z. M.; Xu, B. *Chem. Commun.* **2004**, 2424−25. Yang, Z. M.; Gu, H. W.; Fu, D. G.; Gao, P.; Lam, K. J. K.; Xu, B. *Adv. Mater.* **2004**, *16*, 1440−44.
(10) *Molecular and cellular foundations of biomaterials*; Peppas, N. A., Sefton, M. V., Eds.; Elsevier/Academic Press: Amsterdam, 2004.
(11) Hu, B.-H.; Messersmith, P. B. *J. Am. Chem. Soc.* **2003**, *125*, 14298−99.

 10.1021/ja057412y CCC: $33.50

Scheme 1

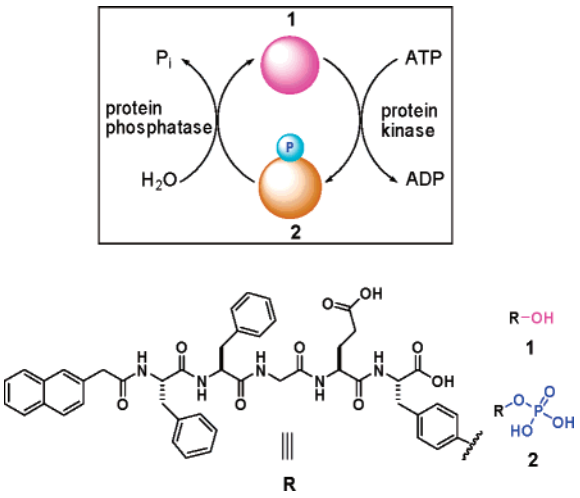

regulate supramolecular hydrogels (e.g., for reversible control of the self-assembly of the hydrogelators) has yet to be explored.

Because most enzymatic reactions are essentially irreversible, a single enzyme hardly ever controls hydrogels in a reversible manner. Nature solves a similar dilemma by using a pair of enzymes that have counteracting activities to switch the functions of proteins.[1] We opt to mimic nature by using a kinase/phosphatase switch to regulate supramolecular hydrogels. As shown in Scheme 1, we synthesize a pentapeptidic hydrogelator, Nap−FFGEY (**1**), which forms hydrogels at 0.6 wt % via the self-assembly of **1**. Adding a kinase to the hydrogel in the presence of adenosine triphosphates (ATP) phosphorylates **1** to give the corresponding phosphate (**2**), thus disrupting the self-assembly to induce a gel−sol phase transition; treating the resulting solution with a phosphatase dephosphorylates **2** to form **1**, thus restoring the self-assembly to form the hydrogel. Moreover, subcutaneous injection of **2** in mice leads to the formation of supramolecular hydrogel in vivo. In addition to being the first demonstration of an enzyme-switch-regulated supramolecular hydrogel and the first formation of supramolecular hydrogels in vivo by an enzymatic reaction, the combination of the kinase/phosphatase switch with supramolecular hydrogels promises a new way to make and apply biomaterials because phosphorylation and dephosphorylation, as common yet important biological reactions, occur in many organisms. Because many diseases (e.g., cancer,[12] diabetes,[13] Alzheimer's disease,[14] and multiple sclerosis[15]) are associated with the abnormal activities of phosphatases and/or kinases,[16] enzyme-switch-regulated hydrogelation, compared with conventional physical and chemical processes, should be superior because it enhances the biologically specific response of the hydrogels regarding the level of enzyme expression. Furthermore, investigation of the enzyme-switch-regulated self-assembly of hydrogelators helps us to understand the functions of supramolecular hydrogels in a biological environment where multiple enzymes exist.

Results and Discussions

Design and Synthesis. We design Nap−FFGEY (**1**, Scheme 1) as both the kinase substrate and the hydrogelator because (i) FF is prone to self-assembly,[17] (ii) Nap−FF gels water effectively (at 0.8 wt %[18]), and (iii) the residue of Glu-Tyr (EY) accepts phosphorylation in the presence of a tyrosine kinase.[19] One of the motivations to use naphthalene (Nap) rather than *N*-(fluorenyl-methoxycarbonyl) (FMOC) is that Nap should be more biocompatible, as evidenced by several clinical drugs consisting of a Nap motif (e.g., propranolol, naphazoline, nafronyl). We choose to use glycine (G) to connect Nap−FF with EY because glycine is the simplest amino acid. Unlike other pentapeptides,[4] FFGEY is not a known epitope of any protein, but it carries the basic structural requirement to serve as the substrate of the tyrosine kinase. After obtaining **1** through solid-phase synthesis,[20] we tested the hydrogelation ability of **1**. Via a slight adjustment of pH (from 7.8 to 7.5), **1** forms a transparent hydrogel in water at 0.6 wt %.[20] The successful hydrogelation of **1** implies that Nap−FF also may act as a useful motif to conjugate with other amino acid residues to construct hydrogelators.

Enzyme Switch Controls the Phase Transition of the Hydrogel. After confirming that **1** is indeed an efficient hydrogelator, we examined the use of the kinase/phosphatase switch to control the phase transition of the hydrogel. The addition of **1** (3 mg) into a buffer (0.5 mL, containing 10 mM of ATP) creates a transparent hydrogel (gel I, Figure 1A) in 5 min. Then, 3 U of tyrosine kinase (50 μL) was added on the top of gel I to initiate the phosphorylation of **1**. After 24 h, gel I turned into a clear solution (Figure 1B). An HPLC test of the solution confirmed that ~46% of **1** was converted to **2**. Because the phosphate groups of **2** repel each other to weaken the self-assembly of the nanofiber and render **2** more hydrophilic than **1**, the gel−sol phase transition occurs. The addition of ~200 U of alkali phosphatase (10 μL) into the solution restores the hydrogel (gel II, Figure 1C) in 1 h. After another 4 h, HPLC analysis showed that 99.1% of **2** transformed back to **1**. Because the catalytic activity of the phosphatase used in this experiment is about 1000 times higher than that of kinase, we are able to complete one cycle of the gel−sol−gel transformation. To cycle such a transformation many times, one might need to adjust the relative amounts of a pair of enzymes that have similar activities. Nevertheless, the result demonstrated here validates the concept of the regulation supramolecular hydrogels by an enzyme switch. In addition, the new insight of the dynamic cell signaling suggests that a stimulus tips the protein kinase (PK)/protein phosphatase (PP) balance by simultaneously activating PKs and deactivating PPs.[16] This model implies that it would be easier to cycle the phase transition of the supramolecular hydrogel in vivo using proper hydrogelators as the substrates, which may lead to a drug delivery system that responds to biological activities of tissues.

(12) Kikuchi, K.; Nakamura, K.; Shima, H. *Curr. Top. Biochem. Res.* **1999**, *1*, 75−87.
(13) Hutton, J. C.; Eisenbarth, G. S. *Proc. Natl. Acad. Sci. U.S.A.* **2003**, *100*, 8626−28.
(14) Eidenmueller, J.; Fath, T.; Hellwig, A.; Reed, J.; Sontag, E.; Brandt, R. *Biochemistry* **2000**, *39*, 13166−75. Yuan, J.; Yankner, B. A. *Nature* **2000**, *407*, 802−9.
(15) Auch, C. J.; Saha, R. N.; Sheikh, F. G.; Liu, X.; Jacobs, B. L.; Pahan, K. *FEBS Lett.* **2004**, *563*, 223−28.
(16) den Hertog, J. *EMBO Rep.* **2003**, *4*, 1027−31.
(17) Kol, N.; Adler-Abramovich, L.; Barlam, D.; Shneck, R. Z.; Gazit, E.; Rousso, I. *Nano Lett.* **2005**, *5*, 1343−46. Reches, M.; Gazit, E. *Science* **2003**, *300*, 625−27.
(18) Yang, Z.; Xu, B. Unpublished results, 2005.
(19) Latour, S.; Veillette, A. *Curr. Opin. Immunol.* **2001**, *13*, 299−306.
(20) Supporting Information.

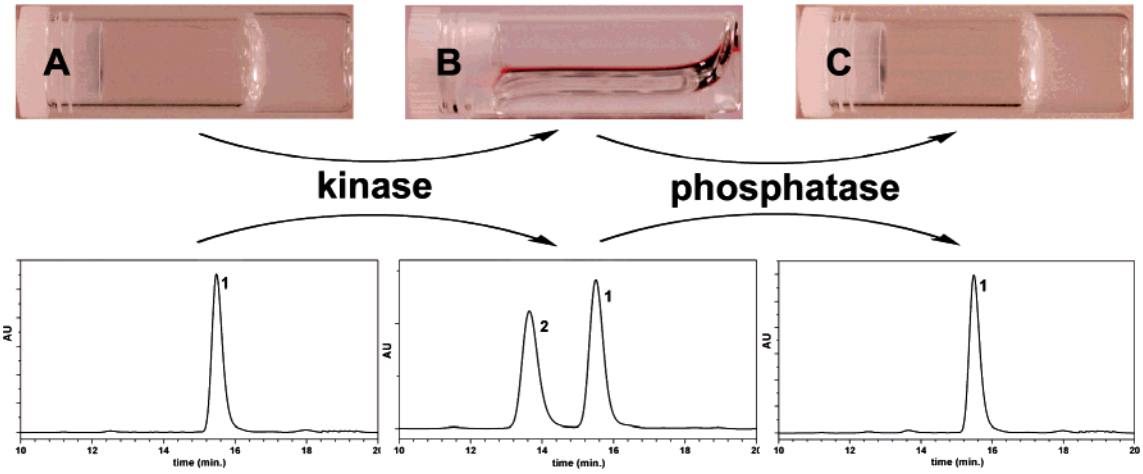

Figure 1. Optical images and corresponding HPLC traces of (A) gel I; (B) the solution obtained after adding a kinase to gel I; and (C) gel II. The hydrogels are on the right side of the panels (A, C), viewing from the bottoms of the vials. The solution containing **1** and **2** in almost 1:1 ratio forms a meniscus in the tilted vial (panel B).

Rheological Study. To evaluate the viscoelastic properties of the gel, we first used dynamic strain sweep to determine the proper condition for the dynamic frequency sweep of gel I. As shown in Figure 2A, the values of the storage modulus (G′) and the loss modulus (G″) exhibit a weak dependence from 0.1 to 1.0% of strain (with G′ dominating G″), indicating that the sample is a hydrogel. After setting the strain amplitude at 0.8% (within the linear response regime of strain amplitude), we used dynamic frequency sweep to study gel I. Figure 2B exhibits that G′ and G″ slightly increase with the increase of frequency from 0.1 to 100 rad/s. The value of G′ is about five times larger than that of G″in the whole range (0.1−100 rad/s), suggesting that gel I is fairly tolerant to external force.

To study the enzymatic formation of gel II, the mode of dynamic time sweep was chosen to examine the change of viscoelasticity of the solution containing **1** and **2** in a ratio of 1:1 upon adding the phosphatase. Alkali phosphatase (400 U/mL) was added to the solution of 0.3 wt % of **1** and 0.3 wt % of **2** in the buffer for the rheological measurement. As shown in Figure 2C, G′ and G″ of the mixture are very small at the moment of the addition of the enzyme, indicating that the solution of **1** and **2** indeed behaves as a low-viscosity liquid when **1** and **2** are in equal amount. Thereafter, both G′ and G″ increase with time, and the value of G′ starts dominating G″ in about 30 min after the addition of the phosphatase, suggesting the approach of the gelling point. After 1.5 h, the plateau value of G′ is about 10 times larger than that of G″, indicating the extensive formation of a three-dimensional matrix in the hydrogel. The time needed to reach the gelling point is shorter than that of a free-standing sample (about 1 h), likely because mechanical perturbations associated with rheological measurements also accelerate the dephosphorylation reaction catalyzed by the enzyme.

Morphological and Spectral Studies. Because they are formed via different processes, gels I and II offer a fine opportunity to evaluate the influence of the enzyme on the self-assembly process. According to the cryo-TEM images of the gels (Figure 3), **1** self-assembles into nanofibers of various sizes in gel I (with the diameters of 28 ± 5 nm) and into uniform nanotubes in gel II (with diameters of 18 ± 1.5 nm and wall thicknesses of 6 nm), indicating that the enzyme switch regulates the self-assembly process to afford better nanofibers. Two factors likely contribute to the kinetics of self-assembly to give the better defined fibers in Figure 3B. First, compared to the change of pH to afford gel I in Figure 3A, the dephosphorylation of **2** by the phosphatase allows the nanofibers to form more slowly, thus permitting a more ordered self-assembled nanostructure. Second, because the enzyme pair catalyzes both phosphorylation and dephosphorylation during the formation of gel II, we speculate that the tyrosine kinase probably phosphorylates the disorder regions in the nanofibers more easily than it does to the ordered regions. So, the kinase helps to remove the disorder parts by converting **1** to **2**, and the phosphatase transforms **2** back to **1** for reassembly. This equilibrium helps to remold the nanofibers into more uniform nanotubes. In that sense, the enzyme switch helps to reject defects in the self-assembly process for forming the nanotubes of **1** in gel II.

To understand the behavior of **1** below minimum gelation concentration and at the stage shown in Figure 1B, we also used TEM to examine the morphology of the cryo-dried solution of **1** (0.3 wt %) and the solution containing **1** (0.32 wt %) and **2** (0.28 wt %). As shown in Figure 3C and 3D, TEM confirms that there is no extensive formation of nanofibers in both cases except mainly amorphous solids and a small amount of short fibrous structures, suggesting that the concentrations of the hydrogelator in these two conditions are too low to self-assemble into a network of nanofibers for hydrogelation. This result is also consistent with the rheological behavior of the solution containing a 1:1 mixture of **1** and **2**.

To further understand the molecular arrangement of the hydrogel of **1**, we measured the circular dichroism and emission spectra of gels I and II. The CD spectra (Figure 4A) of gels I and II are almost identical, and both exhibit a positive band near 196 nm ($\pi\pi^*$ transition), a negative band near 215 nm ($n\pi^*$ transition), and a negative band near 287 nm ($\pi\pi^*$ of naphthyl aromatics), coinciding with the CD spectra of the nanofibers of oligopeptides[6] and indicating β-sheet features. The fluorescent spectra (Figure 4B) show a peak centered at 338 nm for the solution of **1** and asymmetric peaks with the maximum at 340 nm for gel I and at 342 nm for gel II,[20] indicating monomeric naphthalene moieties. Although the lack of a significant excimer peak of naphthalene (about 450 nm[21])

(21) Ikeda, H.; Iidaka, Y.; Ueno, A. *Org. Lett.* **2003**, *5*, 1625−27.

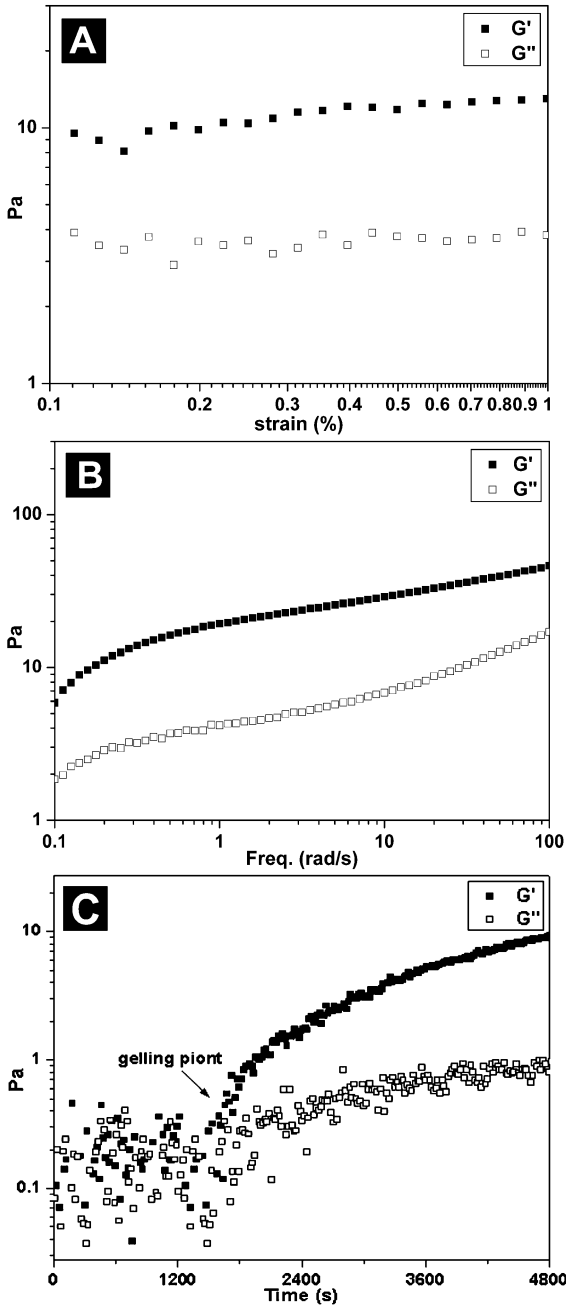

Figure 2. (A) Dynamic strain sweep of gel I at the frequency of 1.0 rad/s; (B) dynamic frequency sweep of gel I at the strain of 0.8%; and (C) dynamic time sweep of the solution containing 0.3 wt % of **1**, 0.3 wt % of **2**, and 400 U/mL of alkali phosphatase in the buffer at the strain of 0.8% and the frequency of 1 rad/s.

excludes the strong $\pi-\pi$ interactions between naphthalene groups in gels I and II, the small broad shoulders above 400 nm indicate weak $\pi-\pi$ interactions between the phenyl and naphthyl groups. This result also agrees with the crystal structure of Nap−FF.[20]

Molecular Arrangements. On the basis of the TEM, CD, and fluorescence spectra of the hydrogel of **1** and the X-ray structure of Nap−FF, we propose the molecular arrangement of **1** in the nanotubes: the hydrogen bonds and hydrophobic interactions (Figure 5A) cooperatively induce the self-assembly of **1** to yield supramolecular polymers, whose molecular packing (Figure 5B) exposes the donors and acceptors of the hydrogen bonds that originate from Glu-Tyr fragments (Figure 5C) and

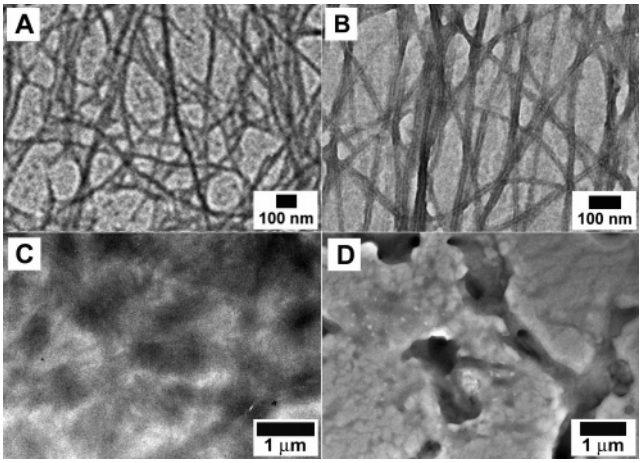

Figure 3. TEM images of the cryo-dried (A) gel I; (B) gel II; (C) solution of **1** (0.3 wt %) in the buffer; and (D) solution containing **1** (0.32 wt %) and **2** (0.28 wt %) in the buffer.

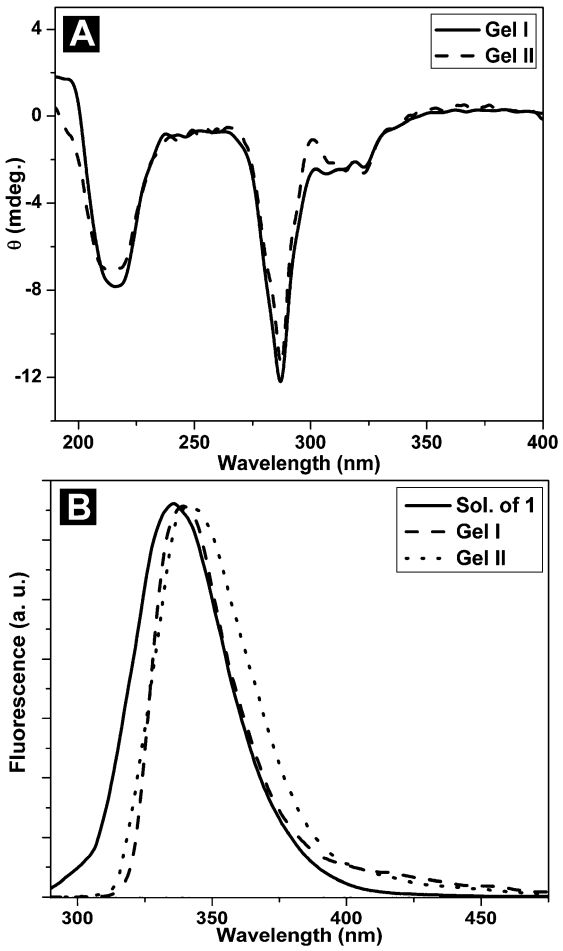

Figure 4. (A) Circular dichroism spectra of gels I and II and (B) fluorescent spectra (λ_{ex} = 272 nm) of solution of **1**, gel I, and gel II.

favors their further aggregation to form nanotubes (Figure 5D). Although it is impossible to rule out entirely other modes of molecular packing, the superstructure depicted in Figure 5 is the most probable one because it conforms to the structures of the NAP−FF segment, complies with the CD and emission spectra of **1** in hydrogels, and allows Glu-Tyr groups to be accessible by the enzymes.

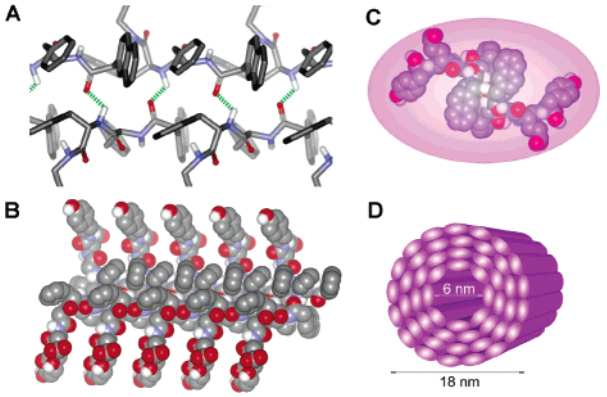

Figure 5. One of the possible molecular arrangements of **1** in nanotubes of gel II: the β-sheet features due to hydrogen bonding (A); the molecular organization of **1** along (B) and crossing to (C) the nanotubes; and the overall molecular packing in the nanotubes (D).

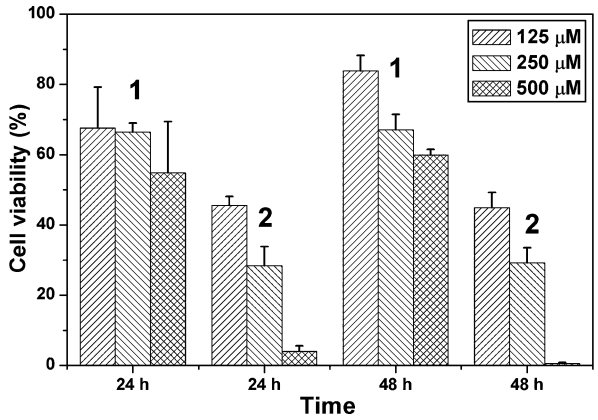

Figure 6. MTT assay on the HeLa cells treated by **1** and **2**.

Biocompatibility of the Hydrogelator and Enzymatic Hydrogelation in Vivo. To verify the biocompatibility of the hydrogelator, we used an MTT assay to examine the cell viability in the presence of **1** or **2**. After 24 h incubation of HeLa cells with **1** and **2**, 68 and 46% of the cells survived at 125 μM of **1** and **2**, respectively. From the results depicted in Figure 6, IC_{50} on the HeLa cell are calculated to be 603 μM for **1** and 93 μM for **2**, respectively. Although **2** at high concentration shows an inhibitory effect on the proliferation of the HeLa cells, the hydrogelator (**1**) is highly biocompatible. The biocompatibility of **1** would be expected to play an important role when the hydrogel is used as material for biomedical applications.

After the preliminary cytotoxicity test confirmed that **1** was biocompatible, we injected the solution of **2** in mice to evaluate the formation of the supramolecular hydrogel of **1** in vivo. Compound **2** (0.5 mL, 0.8 wt %) was injected into each mouse via a subcutaneous mode (i.e., under the skin) and an intraperitoneal mode (i.e., into the abdominal cavity). After 1 h, we observed that the hydrogel formed at the location of subcutaneous injection (Figure 7A). HPLC analysis of the hydrogel reveals that 80.5 $\pm$ 1.2% of **2** turns into **1** (Figure 7C), which is responsible for the hydrogelation. Although no hydrogel forms in the abdominal cavity, an HPLC test of abdominal fluid indicates that 86.2% of **2** changes back to **1** (Figure 7D). By comparing HPLC traces in Figure 7C,D with the HPLC traces of **1** and **2** with known concentrations, we estimated the total amount of compounds (both in **2** and **1**) that remained in the

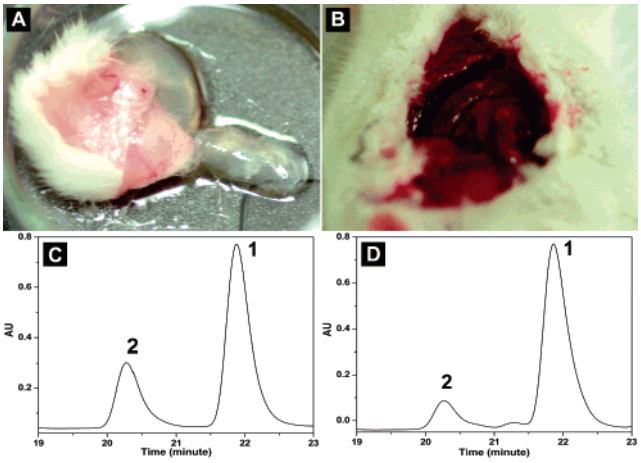

Figure 7. (A) Optical image of the hydrogel formed subcutaneously 1 h after injecting **2** into the mice; (B) the optical image of the abdominal cavity of a mouse 1 h after the injection of **2**; (C) HPLC trace of the hydrogel shown in Figure 7A; and (D) HPLC trace of the abdominal fluid 1 h after injecting **2**.

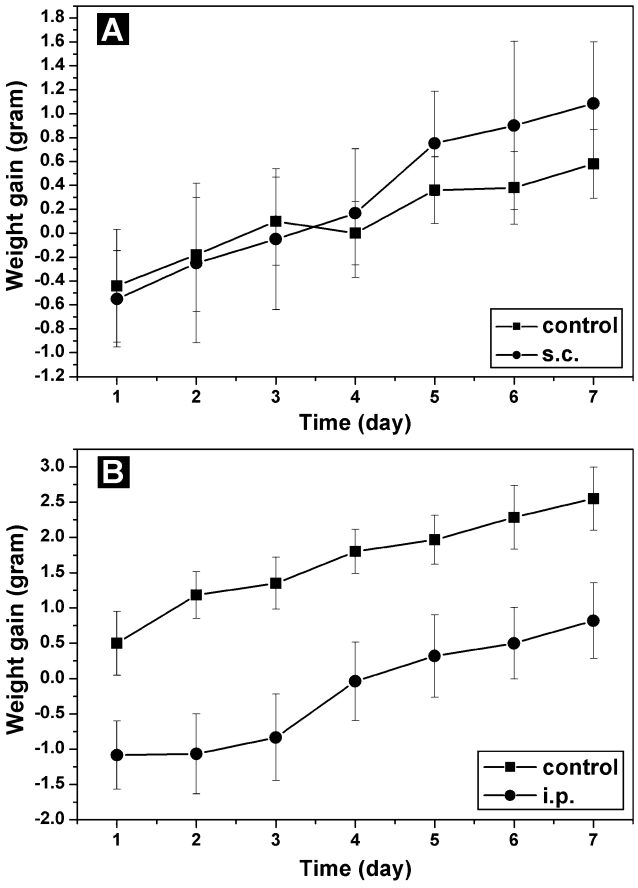

Figure 8. Weight gain of the mice (n = 6, initial body weight = 20 $\pm$ 2 g) after (A) subcutaneously and (B) intraperitoneally injecting 0.5 mL of **2** at 0.8 wt % concentration. Saline solution (0.5 mL) served as the controls for both modes of injection.

site of injection relative to the initial amount of **2** injected. For the subcutaneous injection, the value is about 88.4%; for the intraperitoneal injection, the value is about 76.8%. These results suggest that it is crucial to restrict the diffusion of the precursor of the hydrogelator in tissues or organs to ensure the enzymatic hydrogelation in vivo.

We also monitored the weight change of the mice after injecting **2** to assess the in vivo cytotoxicity of **2**. As shown in

Figure 8A, the mice that received subcutaneous injection of **2** (0.5 mL, 0.8 wt %) lost body weight (mean = 0.55 g, 2.8% decrease) in the first day and so did the mice in the control group (mean = 0.44 g, 2.2% decrease). The two groups of mice both started to gain body weight after the second day. The weight loss and gain of the mice in the two groups remained statistically the same, suggesting that subcutaneous administration of **2** at the experimental dosage results in little acute toxicity to the mice. As shown in Figure 8B, the mice that received intraperitoneal injection of **2** (0.5 mL, 0.8 wt %) lost weight (mean = 1.1 g, 5.5% decrease) in the first day whereas the mice in the control group gained weight (mean = 0.50 g, 2.5% increase). The two groups of mice, however, had almost the same rate of weight gain (0.34 g/day) from the second day to the seventh day. This result indicates that although the intraperitoneal administration of **2** at the experimental dosage results in acute toxicity in the first day the conversion of **2** to **1** reduces the toxicity remarkably after 24 h. The different responses regarding the injection sites are consistent with the amount of **2** diffused away from the injection sites and the in vitro cytotoxicities of **1** and **2**. Being confined in the subcutaneous site, only a small amount of **2** can circulate into the blood and distribute to organs and other tissues, thus lowering the acute toxicity in vivo significantly for subcutaneous injection. Because **2** transforms to **1** eventually, no long-term in vivo toxicity of the hydrogelator is observed for intraperitoneal injection.

Conclusion

In summary, we have demonstrated the use of enzymes to regulate formation/dissociation of self-assembled nanostructures and the corresponding macroscopic transition in a supramolecular hydrogel. The successful in vivo enzymatic hydrogelation suggests that this strategy may allow minimal invasive delivery of the hydrogels in the form of liquid precursors by syringes and needles, renders the hydrogels to bear a desirable response in a biological environment, offers precise control at the molecular level, and promises a new means to engineer biomaterials.

Acknowledgment. This work was partially supported by RGC (Hong Kong) and HIA (HKUST).

Supporting Information Available: Synthesis of **1** and **2**, optical image of the hydrogel of **1** in water, details of in vitro and in vivo assays, and the conditions for HPLC analyses. This material is available free of charge via the Internet at http://pub.acs.org.

JA057412Y